State-of-the-art and evolution of UFSD sensors design at FBK

R. Arcidiacono[b,a,*], G. Borghi[f,g], M. Boscardin[f,g], N. Cartiglia[a], M. Costa[d], G.F. Dalla Betta[e,f], F. Fausti[a], M. Ferrero[b], F. Ficorella[f,g], M. Mandurrino[a], S. M. Mazza[c], E. J. Olave[a], L. Pancheri[e,f], G. Paternoster[f,g], H-F W. Sadrozinski[c], V. Sola[a,d], A. Staiano[a], A. Seiden[c], F. Siviero[d], M. Tornago[d], Y. Zhao[c]

[a]*INFN, Torino, Italy*
[b]*Università del Piemonte Orientale, Italy*
[c]*SCIPP, University of California Santa Cruz, CA, USA*
[d]*Università di Torino, Torino, Italy*
[e]*Università di Trento, Trento, Italy*
[f]*TIFPA INFN Trento, Trento, Italy*
[g]*Fondazione Bruno Kessler, Trento, Italy*

Abstract

In the past few years, there has been growing interest in the development of silicon sensors able to simultaneously measure accurately the time of passage and the position of impinging charged particles. In this contribution, a review of the progresses in the design of UFSD (Ultra-Fast Silicon Detectors) sensors, manufactured at the FBK (Fondazione Bruno Kessler) Foundry, aiming at tracking charged particles in 4 dimensions, is presented. The state-of-the-art UFSD sensors, with excellent timing capability, are planned to be used in both ATLAS and CMS experiments detector upgrade, in order to reduce the background due to the presence of overlapping events in the same bunch crossing.

The latest results on sensors characterization including time resolution, radiation resistance and uniformity of the response are here summarized, pointing out the interplay between the design of the gain layer and the UFSD performances. The research is now focusing on the maximization of the sensor fill factor, to be able to reduce the pixel size, exploring the

*Corresponding author
Email address: roberta.arcidiacono@cern.ch (R. Arcidiacono)

Preprint submitted to Nuclear Instrumentations and Methods in Physics Research A March 26, 2020

implementation of shallow trenches for the pixel isolation and the development of resistive AC-coupled UFSD sensors. In conclusion, a brief review on research paths tailored for detection of low energy X-rays or for low material budget applications is given.

Keywords: silicon sensor, fast timing, low gain, charge multiplication, LGAD

---

1. Introduction

The UFSD project, born as an ERC[1] supported project in 2015, aims at developing silicon detectors for 4D tracking with excellent time and space resolution, able to achieve concurrently a time resolution of the order of tens of ps, and a space resolution $\approx$ tens of μm. The sensor technology used as baseline are Low Gain Avalanche Diodes (LGAD), an evolution of the n-on-p planar silicon sensor incorporating a low (10-30 range), controlled gain in the signal formation mechanism [1]. The charge multiplication conditions, where electrons and holes acquire sufficient kinetic energy to generate additional e/h pairs (electric field E$\sim$300 kV/cm), are obtained by implanting a layer of acceptors with appropriate charge density ($\rho_A \sim 10^{16} cm^3$) below the *n-p* junction, the so-called gain layer. The key points of LGADs optimized for timing are: signals large and fast enough to assure excellent timing performance while maintaining almost unchanged levels of noise (low jitter term), reduced Landau fluctuations ($\approx$ 50 microns thin sensors), and a very uniform weighting field. A detailed description of the UFSD characteristics can be found in [2, 3].

Whithin the UFSD project, the FBK Foundry started developing LGADs in 2016. Since then, four productions of 50-micron thin UFSDs have been completed, covering several aspects of R&D work necessary to reach the project goal performances, including the radiation hardness of the sensors, which should match the requirements of the future High Luminosity Large Hadron Collider (HL-LHC) experiments.

---

[1] ERC GRANT 669529

2. UFSD sensors: key performances

In this section, an overview of performances of the latest UFSD productions is reported, covering the topics on gain uniformity, radiation hardness an time resolution. To be noticed that the typical pad size of the state-of-the-art LGAD is of the order of 1-3 mm^2. The roadmap towards fine-segmented LGADs, able to measure also the position of the traversing particle with high resolution, can be found in sec. 3. It is worth mentioning that the latest UFSD production (*UFSD3*) was partially affected by early breakdown of some devices, and by anomalous high random noise, which made some measurements more challenging. The root cause was understood to be a combination of aggressive pad termination designs and incorrect p-stop doping concentration. An internal FBK run was dedicated to the study of the problem, and the identification of the correct p-stop dose range was achieved.

2.1. The uniformity of the gain

A key parameter for the feasibility of detectors with large area UFSD sensors is the gain layer doping uniformity: a difference a 1% in doping concentration moves the optimum biasing point by ∼11-15 V depending on the gain layer doping profile. It is important to keep the non-uniformity below 1% on a single device, to have comparable performance on the area of the sensor, and below a few percent (the lower, the better) on the whole production, to have sensors that behave similarly and able to share the bias voltage with neighbouring sensors, in case it is needed by the biasing scheme.

The gain uniformity of several wafers of the last FBK production has been tested, measuring C(V) curves for many pads and analyzing the $1/C^2$(V) functions. The voltage at which the gain layer is depleted, V_{GL}, is proportional to the amount of active acceptor density N_A in the gain layer itself (see [4] for more details on this method). The relative spread observed in V_{GL} is a measure of the non-uniformity of the gain layer, and it is found to be 2-3% over the whole production, and less than 2% when excluding sensors at the periphery of the wafers.

2.2. On radiation hardness

Previous studies have demonstrated that neutrons and charged hadrons irradiations, among other well known effects on the silicon substrate, reduce the gain value of the LGADs, changing the way they behave. This effect is due to the initial acceptor removal mechanism that progressively deactivates the acceptors of the gain layer. The initial acceptor removal can be parametrized as $\rho_A(\Phi) = \rho_A(0)e^{-c\Phi}$, where Φ is the irradiation fluence [cm^2], $\rho_A(0)$ ($\rho_A(\Phi)$) the initial (after a fluence Φ) acceptor density [cm^3], and c [cm^2] is the *acceptor removal coefficient* that depends on the initial acceptor concentration $\rho_A(0)$ and on the type of irradiation [4].

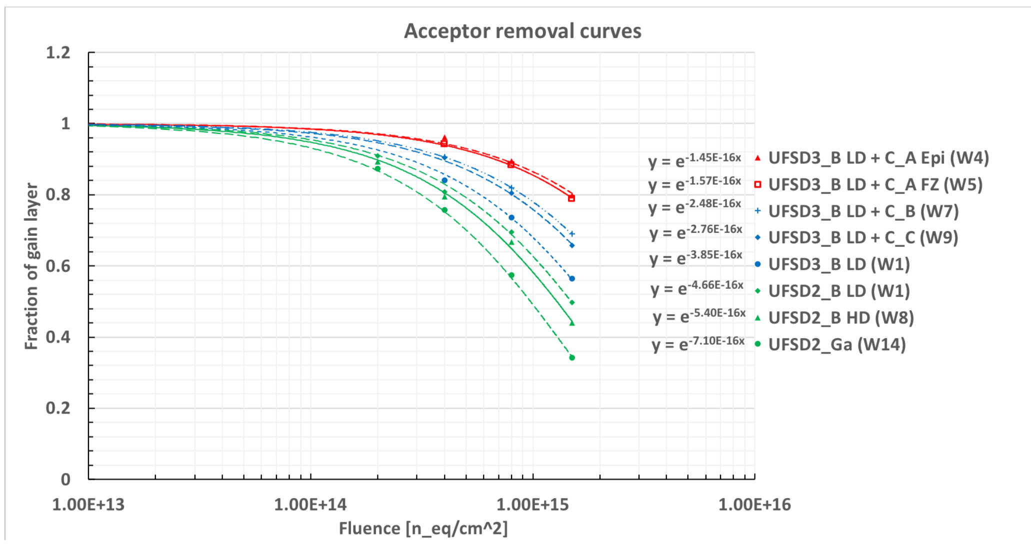

Figure 1: Fraction of gain layer (active acceptor density) as a function of the irradiation fluence received, for UFSD sensors belonging to the UFSD3 production, differing in gain layer design. Data points are superimposed with an exponential fit $y = e^{-\mathbf{c}x}$. Smaller coefficient **c** leads to more radiation resistant gain layers. For reference, a few sensors from the UFSD2 production are shown.

A great effort has been put, in the past three years, to enhance the radiation hardness of the gain layer, exploring different solutions for the gain layer design (varying doping profile/type of acceptor, co-implanting carbon). Extensive irradiation campaigns allowed to study the radiation hardness of the various designs.

Figure 1 represents the fraction of gain layer (active acceptor density) surviving at a given fluence, as a function of the fluence received, for various UFSD3 sensor types. The superimposed exponential fit $y = e^{-\mathbf{c}x}$ is parametrized with the acceptor removal coefficient. A smaller value of the coefficient **c** leads to more radiation resistant gain layers. For reference, a few sensors from the UFSD2 production are also shown (in green). These measurements demonstrate that: *(i)* the gain layer produced in Low Diffusion (LD - narrower layer profile) is more radiation resistant than the High Diffusion (HD) type; *(ii)* the co-implantation of carbon in the gain layer volume improves by a factor of ∼2 the radiation resistance; *(iii)* the carbon dose called C_A (a.u.) shows the best radiation resistance (both for Epi and FZ wafer substrate), and increasing the carbon dose by a factor or 2 or 3 (C_B, C_C) does not improve the radiation hardness. The best radiation-hard FBK UFSD device has a LD type of gain layer, co-implanted with a C_A dose of carbon.

2.3. On time resolution

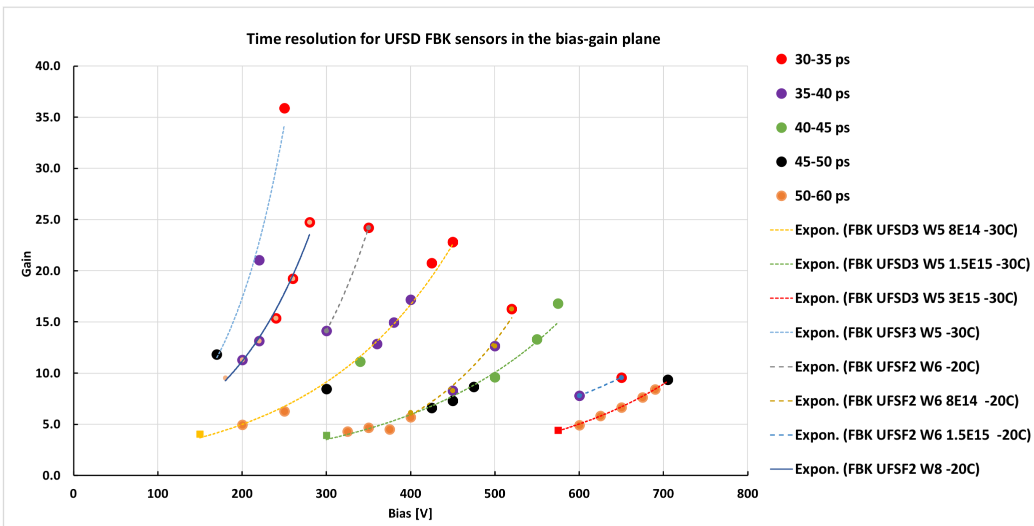

Figure 2: Gain(V) curves of several FBK sensors, new and irradiated at different fluences. The colors around the markers define the time resolution values (in 5 ps range), obtained in laboratory measurements with a β-source, at cold (-20 or -30 °C). The plot shows also how the behavior of a given device changes as a function of the irradiation level.

The time resolution of these devices has been measured with laser systems, for the study of the jitter contribution to the time resolution, with β-source setups in the laboratory, or at beam tests, for a subset of them.

A time resolution in the 25-30 ps range, for 50 microns thick UFSD, has been achieved for new devices with the correct gain layer design, when the sensor is coupled with a fast low-noise pre-amplifier.

The plot shown in fig. 2 gives a comprehensive overview of the state-of-the-art UFSD time performance in relation to the *gain* versus *bias voltage* curve of a given device. Three types of UFSD sensors are represented, new and irradiated up to 3E15 n_{eq}/cm^2. In particular, the plot shows the Gain(V) curves of the three selected devices, with colors around the markers defining the time resolution measured (in 5 ps range), as obtained with the very same β-source setup, at cold (-20 or -30 °C). The three devices differ one another for the gain layer design (doping concentration and profile). As expected, the irradiated sensors are able to reach a given gain for progressively higher bias voltages. For two out of three, it is possible to reach a 30-35 ps time resolution when biased high enough (the gain being high enough to nearly saturate the holes' drift velocity). The UFSD3 W5 device irradiated at 1.5E15 n_{eq}/cm^2 does not reach the expected performance due to random noise at high voltage affecting this production, as previously explained.

2.4. Near future developments

FBK is currently working on the next UFSD production (*UFSD3.2*), which is expected to be completed in Spring 2020. The production is partially dedicated to the CMS and ATLAS timing layer detector upgrades, providing small-scale prototypes, and it will also address a number of optimization studies, including *i)* the exploration of lower carbon dose to be co-implanted in the gain layer, to improve the radiation hardness, *ii)* the fabrication of deep gain layer implant combined with carbon, to improve the operating parameters in highly irradiated devices, and *iii)* the study of aggressive interpad designs, to reduce the no-gain area.

3. Towards fine-segmented LGADs

In the current UFSD design, the area between read-out pads is hosting a Junction Termination Extension (JTE) on each side to contain the gain layers of the two adjacent pads, separated by a p-stop area for the electrical isolation of the pads (a p-type material implantation with a certain pattern). This design leads to a no-gain area for signal collection, due to the nominal distance between the two gain layers, and to an extra periphery of the gain implant where the charges are collected by the JTE and do not pass through the gain layer. The measured width of the no-gain area in state-of-the-art devices ranges between 40 and 75 microns, depending on the producer. The shortest distance achieved in fully working FBK UFSD sensor is 38 microns.

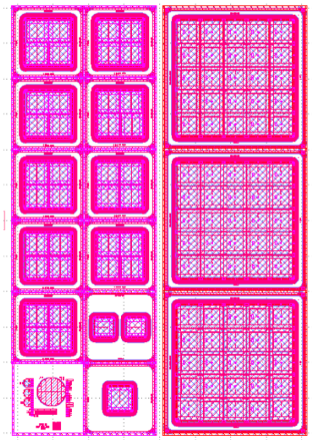

Figure 3: Layout of the UFSD3.2 photo mask, hosting single pads, 2×2 and 5×5 matrices with 1.3×1.3 mm^2 pad size.

The size of the inter-pad no-gain area has an impact on a sensor array fill factor, defined as the ratio of a pixel's particle sensitive area to its total area. As an example, a no-gain area of 40 microns leads to a fill factor of 94% (36%) for a 1.3 mm (100 microns) pitch sensor array.

TCAD simulations performed on UFSD sensors (50 microns thick) show that a no-gain area of about 20 microns could be reached with aggressive designs. Two new technological developments, the Trench-Isolated LGAD (TI-LGAD FBK) and the Resistive AC-coupled LGAD (RSD project), aim at the maximization of the sensor fill factor.

3.1. Trench-Isolated LGADs

The Trench-Isolated LGAD (TI-LGAD) is a technological development of the standard thin LGAD, which implements a different strategy in the pad electrical isolation, to reduce the no-gain area between pads. The standard LGAD inter-pad design is substituted by shallow trenches, less than a 1 μm wide, dug with deep reactive ion etching technique and filled with silicon oxide (Deep Trench Isolation technology). This fabrication process could lead to a nominal no-gain region of a few microns.

The first internal FBK run to study this novel design was produced in 2019. Several wafers with different layouts were processed, changing several fabrication parameters. Each wafer hosts, among other types, 2×1-pixel devices (250 μm $\times$ 375 μm) with single- and double-trench isolation. Figure 4 shows a sketch of the inter-pad region of a single trench TI-LGAD, and a view of the wafer layout for the 2-pixel device. The initial characterization of the production shows that the pixels are electrically isolated, the breakdown voltage and the gain-voltage curves are as in the homologous LGADs. More details can be found in [5].

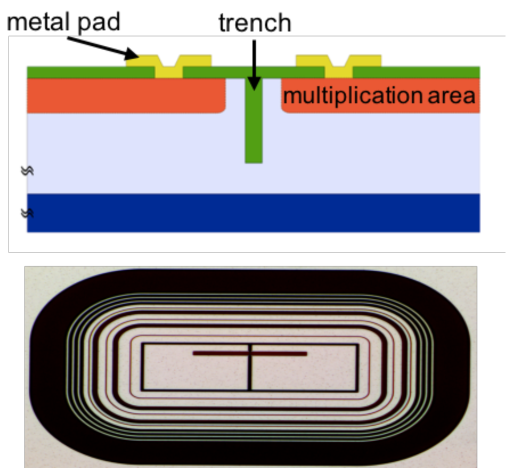

Figure 4: Sketch of the inter-pad region of a single trench TI-LGAD, with the trench (green) visible between the two multiplication regions of the two pixels, followed by a view of the wafer layout for the 2-pixel device. A thin metal opening traversing the inter-pad region is clearly visible.

The width of the no-gain region has been measured using a TCT setup, shooting the laser along the optical window crossing the inter-pad region. The results obtained so far on a few devices are very promising. In fig. 5, a comparison between the best UFSD device and a 2-trench TI-LGAD, both biased at 300 V, is shown. The plot represents the charge collected by two adjacent pads, read out simultaneously during the laser scan, as a function of the position of the laser along the scan line: the collected charge read out in the two channels of the UFSD device is shown in black, while the collected charge of the 2-trench TI-LGAD in blue. The measured inter-pad no-gain distance are 38 μm and 7 μm respectively. The plot also demonstrates the extremely good pad isolation in both types of devices.

Finally, preliminary results on noise level at high voltage and on time resolution are in line with the expectations. Extensive studies of the full production is still ongoing. Several devices have been sent to an irradiation facility, to study the behavior of the trenches when irradiated up to fluences of 3E15 n_{eq}/cm^2.

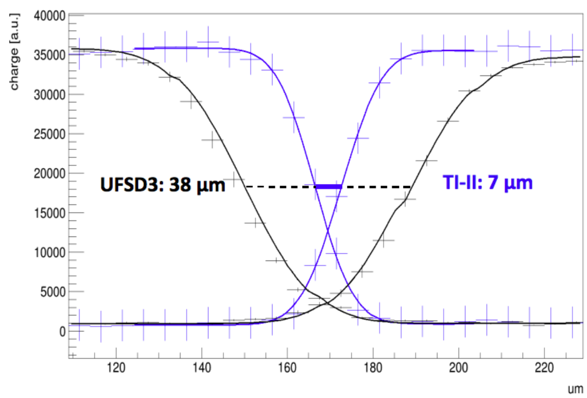

Figure 5: Charge collected by two adjacent pads, read out simultaneously, as a function of the position of the laser during a TCT scan: in black the charges collected for an UFSD device, in blue the charges collected for a 2-trench TI-LGAD. Both devices are biased at 300 V. The measured no-gain area are 38 μm and 7 μm respectively.

3.2. Towards an 100% fill factor: the Resistive AC-coupled LGAD

The Resistive AC-coupled LGAD (RSD) is designed as a device with an intrinsic 100% fill factor: it is a thin LGAD with one continuous gain layer, where the segmentation of the sensor is defined by the read-out pads pattern. The gain layer is separated from the electrodes by a resistive sheet and a capacitive dielectric layer (see Fig.6).

The first FBK RSD production, delivered in mid 2019, comprises of 15 wafers with different splits in key parameters such as *(i)* the resistive sheet dose and the oxide thickness, which have a direct impact on the signal amplitude, discharge time and charge sharing, and *(ii)* the gain dose, which determines the multiplication factor and thus the signal slew rate. Several types of devices have been designed, to explore a wide range of possible pitch/AC-pad-size configuration or targetting a specific application. Extensive electrical characterization and quality control of the production have been performed, together with detailed studies of the RSD signal formation using a Transient Current Technique (TCT) setup [6].

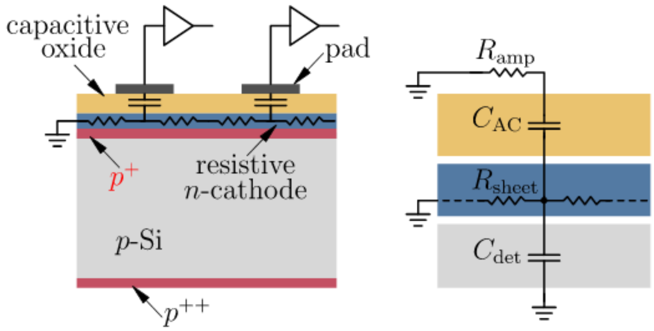

Figure 6: Schematic cross-sectional view of an RSD device, where the continuous gain layer, the resistive n-type cathode and the capacitive dielectric layer are represented. On the right side, the circuital model of a single read-out pad is shown.

The TCT setup has a IR laser ($\lambda = 1064$ nm) with a spot size of 10 μm and the possibility to perform x-y scans with micrometrical precision: this allows to extract very precise information on the RSD signal dinamics. The signals induced by the laser reach their maximum when the impact point is in the middle of the AC pad, and get smaller (and delayed) moving away from the pad, as a function of the distance between the hit point and the read-out pad (more information on the signal formation characteristics can be found in [7]). As a consequence, the signal created by a particle is visible in several pads around the hit point. The characteristics of the charge induced in RSD read-out pads can be thus exploited, with the acquisition of data from more channels at the same time, to obtain excellent space and time resolution.

Extensive tests have been performed in the lab, always using the TCT laser setup, on a set of 3×3 matrices with different pitch/AC-pad-size geometries, in order to develop optimized reconstruction algorithms and evaluate their space and time resolution, in absence of Landau fluctuations of the signal. During these measurements, the device under test is operated at a bias voltage such to have gain=17, and four AC-pads are wire-bonded to a multichannel amplifier board and simultaneously read out. The other pads are grounded. The laser is shot several times on a given point, following a pattern (see red dots in fig. 7, representing a specific device), with an intensity emulating the charge released by one minimum ionizing particle (MIP).

Preliminary results for the space resolution are obtained using, as recon-

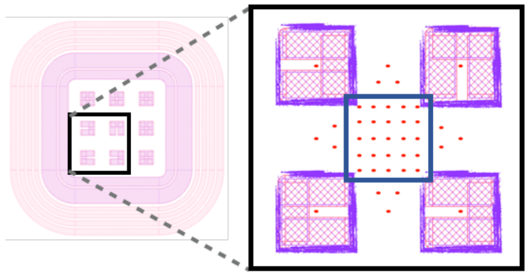

Figure 7: Layout of a 3×3 RSD matrix, with a zoom to the region covered by the TCT laser scan, represented by the red dots. Only the points included in the squared area between the four read out pads have been analysed.

struction algorithm for the hits' coordinates, an amplitude-weighted centroid of the coordinates of the four read out channels. The reconstructed hit positions x_{reco}, y_{reco} are then compared with the well known coordinates of the laser moving stage. The space resolution is quantified by the standard deviation of the distribution obtained plotting the difference $x_{laser} - x_{reco}$ (or the equivalent for the y coordinate) for a large number of events (~ 500 per point). To ensure an unbiased analysis, only the events where the charge induced was well sampled by the four connected pads have been selected: only the laser scan points located in the central squared area between the pads have been used, with the further request on the signal amplitudes to be >10 mV.

Figure 8 shows the distribution of the $x_{laser} - x_{reco}$ differences, overlaid with a guassian fit, for three types of RSD geometry: the 50 microns AC-pad size with 100 microns pitch (50-100 for brevity), the 100-200 and the 200-500 types. The measured space resolution is of the order of 6 μm for the 50-100, 100-200 types, and ∼20 μm for the 200-500 type. These results should be considered preliminary, but they definitely point to a much improved space resolution w.r.t traditional pixelated silicon devices (typically pitch/$\sqrt{12}$).

The time resolution has been measured using the same set of data with identical selection criteria. The time of the hit t_{hit} is reconstructed as an amplitude-weighted centroid of the time of the maximum amplitude t'_{max} seen by the four read out pads. The quantity t'_{max} is actually the time of the maximum corrected for two effects: *(i)* the delay due to propagation time of the signal from the impact position to the read-out pad, which is proportional to the hit position-pad distance, and *(ii)* a time offset due to the difference introduced by the whole read-out chain. The measurement of the hit position is thus used to correct the t_{max} for the propagation delay, and a mis-computed hit position will also affect the time measurement. The time resolution is quantified by the standard deviation of the $t_{trigger} - t_{hit}$ distribution, for a large number of events, where $t_{trigger}$ is the time given by the laser system.

Figure 9 shows the distribution of the $t_{trigger} - t_{hit}$ differences, overlaid with a guassian fit, for the three 50-100, 100-200 and 200-500 RSD geometries (AC-pad size - pitch). The time resolution obtained with the above mentioned method is $\sigma_t \sim 17$ ps, 24 ps and 31 ps for the 50-100, 100-200 and 200-500 respectively. These results should be considered preliminary.

It is important to note that eventual differences of the acquisition chain lead to unequal response to the same input charge: the preliminary calibration of the amplifiers used in these measurements can be optimized to eliminate the offsets currently affectiing some of the central values for the position reconstruction.

Further improvements in the performance may derive from an ongoing analysis, which aims at a sophisticated reconstruction algorithm for the hit position, based on a more accurate description of the propagation/attenuation properties of the AC-resistive sheet. This approach uses *look-up-tables*, geometry dependent, in which the correlation between impact point and charge sharing on the surrounding pads is encoded.

Studies of the RSD behavior with β source particles and at beam test are ongoing.

4. Future developments for low energy X-rays detection

A recently approved three-years R&D project aims at the reduction of the active and of the physical thickness of the LGAD sensors, down to 20-30 microns, and at the implemention of a very thin rear entrance window to the active volume of the device. Such improvements open the way to different fields of application, such as low energy (keV) X-rays detection, and to very low material budget applications. In this project, the reduction of the size of the pad is not at the center of the development work.

Soft X-rays (energy of ~1-10 keV) barely penetrate the silicon volume and release only ~300 electron-hole pairs per 1 keV. The internal gain of the LGADs enables the detection of low charge signals thanks to the intrinsic amplification of the signal ([8]). In order to improve the performance, X-rays

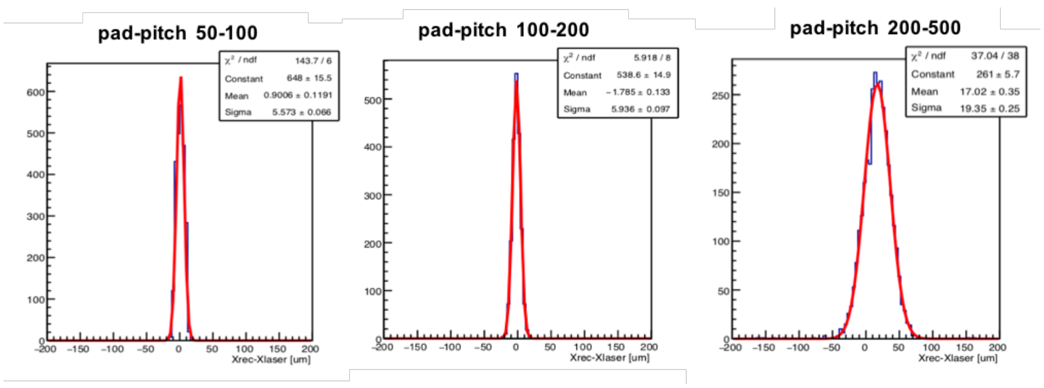

Figure 8: Distributions of $x_{laser} - x_{reco}$, overlaid with guassian fits, for the 50-100, 100-200 and 200-500 RSD geometry types. The measured space resolution is of the order of 6 μm for the 50-100, 100-200 types, and $\sim$ 20 μm for the 200-500 type. Data obtained with a laser TCT setup.

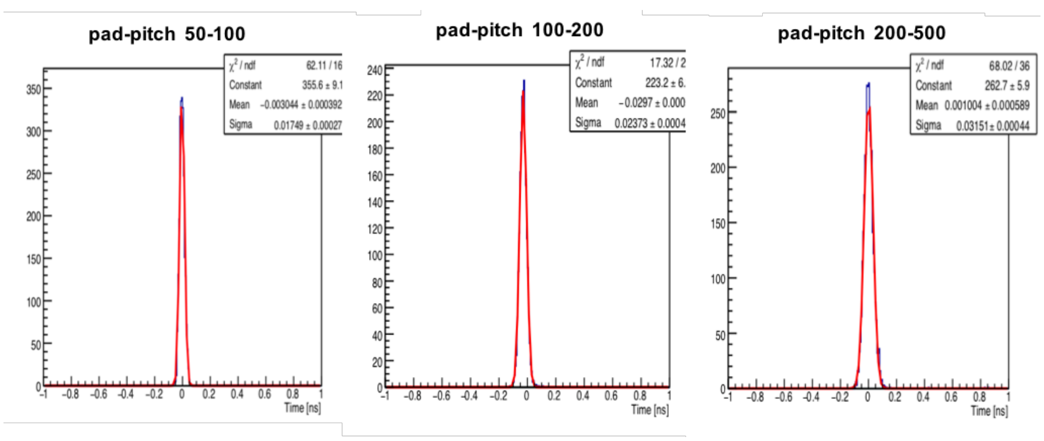

Figure 9: Distributions of $t_{trigger} - t_{hit}$ differences, overlaid with guassian fits, for the 50-100, 100-200 and 200-500 RSD geometry types. The measured time resolution is 17 ps, 24 ps and 31 ps for the 50-100, 100-200 and 200-500 respectively. Data obtained with a laser TCT setup.

should reach the active volume of the sensor through back-illumination on the p-side, in absence of the support wafer. The feasibility of manufacturing LGADs with a double-sided process, having the gain layer on one side and the thin entrance window on the other side, is the key to the success of this work.

5. Conclusion

The UFSD project started in 2015 with the goal of designing sensors suitable for 4D tracking in High Energy Physics experiments. Several productions implementing aggressive or optimized technological solutions have been completed and thourougly studied. The state-of-the-art UFSD sensor has achieved: excellent time resolution ($\simeq$30 ps); very good production uniformity and yield for sensors of $\sim$3 cm^2; optimization of the gain layer design to enhance operating parameters and radiation hardness (time performances mantained up to a fluence of 1.5E15 n_{eq}/cm^2), and an inter-pad no-gain area of $\sim$40 microns. The R&D work to reduce further the inter-pad no-gain area, the limiting factor to the production of matrices with a fine grained pixelation (100's of microns or less), is currently exploring more aggressive pad/gain isolation designs, as well as other technological solutions as trenches to isolate the pad. The latter solution gives inter-pad no-gain region of the order of 5-10 microns. Another very promizing technology, which may represent the best option for 100% fill-factor sensors, is the resistive AC-LGAD (RSD devices), currently still under studies. Preliminary results obtained with a laser source point to time resolutions in the 20-30 ps range and space resolutions better than the pitch/$\sqrt{12}$. We are expecting to have more comprehensive results on the ongoing R&Ds, addressing the detector fill factor, in the next 6 months.

Aknowledgments

We thank our collaborators within RD50, ATLAS and CMS who participated in the development of UFSD. Part of this work has been financed by the European Union Horizon 2020 Research and Innovation funding program, under Grant Agreement no. 654168 (AIDA-2020) and Grant Agreement no. 669529 (ERC UFSD669529), by the Italian Ministero degli Affari Esteri, by INFN Gruppo V and by the Dipartimento di Eccellenza, University of Torino (ex L. 232/2016, art. 1, cc. 314, 337). The work was supported by the United States Department of Energy, grant DE-FG02-04ER41286.

References

[1] G. Pellegrini, et al., Technology developments and first measurements of Low Gain Avalanche Detectors (LGAD) for high energy physics applications, Nuclear Instruments and Methods in Physics Research A 765 (2014) 12–16.

[2] N. Cartiglia, et al., Design optimization of ultra-fast silicon detectors, Nuclear Instruments and Methods in Physics Research A 796 (2015) 141–148.

[3] H. F.-W. Sadrozinski, A. Seiden, N. Cartiglia, 4D tracking with ultra-fast silicon detectors, Reports on Progress in Physics 81 (2) (2018) 026101.

[4] M. Ferrero, et al., Radiation resistant lgad design, Nuclear Instruments and Methods in Physics Research Section A 919 (2019) 16 – 26.

[5] G. Paternoster, et al., Novel strategies for fine-segmented lgads, HSTD12, 2019, proceedings of the 12th International "Hiroshima" Symposium (HSTD12) at Hiroshima, Japan.

[6] M. Mandurrino, et al., Demonstration of 200-, 100-, and 50- μ m pitch resistive ac-coupled silicon detectors (rsd) with 100% fill-factor for 4d particle tracking, IEEE Electron Device Letters 40 (11) (2019) 1780–1783.

[7] N. Cartiglia, et al., Future silicon trackers, HSTD12, 2019, proceedings of the 12th International "Hiroshima" Symposium (HSTD12) at Hiroshima, Japan.

[8] Andrä, et al., Development of low-energy X-ray detectors using LGAD sensors, Journal of Synchrotron Radiation 26 (4) (2019) 1226–1237.